Self-Initiating MUSIC-Based Direction Finding and Polarization Estimation in Spatio-Polarizational Beamspace

Kainam Thomas Wong, *Member, IEEE,* and Michael D. Zoltowski, *Fellow, IEEE*

Abstract—A novel self-initiating multiple signal classification (MUSIC)-based direction-finding (DF) and polarization-estimation algorithm in spatio-polarizational beamspace is herein presented for an arbitrarily spaced array of identically oriented electromagnetic vector sensors. An electromagnetic vector sensor, already commercially available, is composed of six colocated, but diversely polarized, antennas distinctly measuring all six electromagnetic-field components of a multisource incident wave field. This proposed algorithm: 1) exploits the incident sources' polarization diversity; 2) decouples the estimation of the sources' arrival angles from the estimation of the sources' polarization parameters; 3) uses ESPRIT on pairs of vector sensors to self-generate coarse estimates of the arrival angles to start off its MUSIC-based iterative search without any *a priori* information on the incident sources' parameters; 4) estimate the sources' polarization states; and 5) automatically pairs the *x*-axis direction-cosine estimates with the *y*-axis direction-cosine estimates and with the polarization estimates. Monte Carlo simulation results verify the efficacy of the proposed method.

Index Terms—Antenna arrays, array signal processing, data fusion, direction of arrival estimation, polarization.

I. INTRODUCTION

A. Basic Ideas Underlying the New Algorithm

1) What are Electromagnetic Vector-Sensors?:

AN electromagnetic vector sensor consists of six spatially colocated nonidentical nonisotropic antennas, separately measuring the incident wavefield's three electric-field components and three magnetic-field components [10], [12]. An electromagnetic vector-sensor, like other diversely polarized array, can exploit any polarization diversity among the impinging sources. Vector sensors are already commercially available, for example, from Flam and Russell, Inc., Horsham, PA [14][1] and from EMC Baden, Inc., Baden, Switzerland.[2] The former implements the vector sensor concept by colocating three electric dipoles and three magnetic loops in a point-like

[1]The superCART array covers the shortwave band from 2 to 30 MHz.

[2]Operating frequency unknown.

geometry, with a dipole and a loop aligned along each of the Cartesian coordinates. A vector cross product between an incident source's normalized electric-field vector estimate with the source's normalized magnetic-field vector estimate to give the *k*th source's normalized Poynting vector $\boldsymbol{p}_k$: [12]

$$\boldsymbol{p}_k \stackrel{\text{def}}{=} \begin{bmatrix} p_{x_k} \\ p_{y_k} \\ p_{z_k} \end{bmatrix} = \begin{bmatrix} u_k \\ v_k \\ w_k \end{bmatrix} = \begin{bmatrix} \sin\theta_k \cos\phi_k \\ \sin\theta_k \sin\phi_k \\ \cos\theta_k \end{bmatrix}$$
$$= \text{Re}\left\{ \frac{\boldsymbol{e}(\theta_k, \phi_k, \gamma_k, \eta_k)}{\|\boldsymbol{e}(\theta_k, \phi_k, \gamma_k, \eta_k)\|} \times \frac{\boldsymbol{h}^*(\theta_k, \phi_k, \gamma_k, \eta_k)}{\|\boldsymbol{h}(\theta_k, \phi_k, \gamma_k, \eta_k)\|} \right\}$$

(1)

where

*	conjugation;
ϕ_k	*k*th source's azimuth angle;
θ_k	elevation angle;
γ_k and η_k	polarization parameters.

This vector cross-product direction-of-arrival (DOA) estimator, regardless of the array geometry, automatically pairs the estimates of $\{u_k, k = 1, \ldots, K\}$ and $\{v_j, j = 1, \ldots, K\}$ with no further processing. Furthermore, the vector cross-product estimator produces the *z*-axis direction cosine estimates, which allow unambiguous source localization along any spherical direction, rather than the hemispherical region of support customary of planar arrays.

2) Why Use MUSIC?:

Multiple signal classification (MUSIC) [2] is a highly popular eigenstructure-based (i.e., vector subspace-based) direction-finding (DF) method applicable to an irregularly spaced array. MUSIC uses the noise-subspace eigenvectors of the data correlation matrix to form a null spectrum, the minima of which are iteratively estimated to yield the signal parameter estimates. Relative to the optimum maximum-likelihood (ML) parameter estimation method, eigenstructure-based methods: 1) demand less computation; 2) do not require any *a priori* information of the joint probability density relating all sources and noise, but only the noise's second-order statistics; 3) yield asymptotically unbiased and efficient estimates of the DOA; 4) produce at moderate signal-to-noise ratios (SNRs) estimation performance comparable to the optimal methods. Irregularly spaced arrays are widely used, for example, to mount antennas on the body of an airplane or to extend array aperture by spacing array elements over the Nyquist half-wavelength maximum. For arrays with uniform element spacing exceeding the Nyquist

half-wavelength maximum, array designers need to control grating lobes to avoid ambiguity in the DOA estimates.

3) Why Use Spatio-Polarizational Beamspace?: An electromagnetic vector sensor, with its six constituent antennas, may form spatio-polarizational beams (for example, via linearly constrained minimum variance (LCMV) beamforming [1]) to pass only a signal-of-interest along certain angular/polarizational dimensions. Moreover, vector sensor-based beams decouple the DOA-estimation problem from the polarization parameter estimation problem, thus reducing MUSIC's iterative search from four dimensions to two dimensions (over only the azimuth and the elevation). This eliminates many local optima in MUSIC's iterative search and, thus, facilitates more speedy convergence to the global optimum.

4) Self-Initiating MUSIC-Based Iterative Estimation: MUSIC performs an M-dimensional iterative search for K extrema of a scalar function to estimate the M parameters of all K incident sources. Whether this optimization converges to the global optimum and how fast this iterative search converges depend very much on the proximity of the initial parameter values to the true global optimum. Without *a priori* information of the incident sources, initial estimates are generally unobtainable. This new algorithm self-generates its own initial coarse estimates *blindly* without any *a priori* information. The deployment of multiple spatially displaced vector sensors thus allows two separate independent approaches to estimate the DOAs—via the vector cross-product DOA estimator at each electromagnetic vector sensor and via an iterative search (as in MUSIC) over the multivector-sensor array manifold parameterized by the intervector-sensor spatial phase delays. The Poynting vector estimate, obtained by the vector cross-product above, serve here as coarse direction cosine estimates to start off MUSIC's iterative search.

B. Summary of Relevant Literature

This present scheme distinguishes itself from most other beamspace MUSIC algorithms [3], [5], [7] in two regards: 1) beams are formed in the polarization domain besides the spatial domain and 2) these beams are formed *blindly*, with no *a priori* source information. However, if any such *a priori* information is available, it may be incorporated to the present technique.

Many other direction finding algorithms (e.g., [11], [13], [16]) use multicomponent polarization-sensitive sensors; however, they do not separately measure all six electromagnetic-field components of the impinging wavefields and, thus, do not use the vector cross-product DOA-estimator pivotal to the success of the present algorithm. The first direction finding algorithms explicitly exploiting all six electromagnetic components appear to be developed separately in [10] and [12]. Reference [12] introduces the vector cross-product DOA estimator to the signal processing community, proposes the scalar mean square angular error (MSAE) as a performance measure and derives a compact expression and a bound for the asymptotic MSAE. Reference [10] is first to apply ESPRIT to a vector-sensor array, but it does not use the vector cross-product DOA estimator. Reference [10] is simplified in [35] and is extended in [27] for partially polarized sources. Reference [36] is first to use the vector cross-product DOA estimator in an

ESPRIT-based direction finding scheme involving multiple vector sensors and is followed up by [32] and [37]. References [25], [28] apply the vector cross-product DOA-estimator in another ESPRIT-based with a solitary vector sensor. Signal detection using vector sensors are investigated in [17]. Polarimetric modeling using vector sensors are performed in [19]. Identifiability and uniqueness issues associated with vector sensors are analyzed in [9], [20], [21], [23], [24].

II. DATA MODEL FOR IRREGULARLY SPACED ELECTROMAGNETIC VECTOR SENSORS

Completely polarized[3] transverse electromagnetic plane waves, having traveled through a nonconductive homogeneous isotropic medium, impinge upon an array of identically oriented electromagnetic vector sensors located irregularly in a three-dimensional (3-D) region. The kth incident source's electric-field vector $\boldsymbol{e}_k$ and magnetic-field vector $\boldsymbol{h}_k$ may be expressed in Cartesian coordinates as [10], [12]

$$
\boldsymbol{a}\left(\theta_k, \phi_k, \gamma_k, \eta_k\right)
$$

$$
\overset{\text{def}}{=} \begin{bmatrix} \boldsymbol{e}_k \\ \boldsymbol{h}_k \end{bmatrix} \overset{\text{def}}{=} \begin{bmatrix} e_x\left(\theta_k, \phi_k, \gamma_k, \eta_k\right) \\ e_y\left(\theta_k, \phi_k, \gamma_k, \eta_k\right) \\ e_z\left(\theta_k, \gamma_k, \eta_k\right) \\ h_x\left(\theta_k, \phi_k, \gamma_k, \eta_k\right) \\ h_y\left(\theta_k, \phi_k, \gamma_k, \eta_k\right) \\ h_z\left(\theta_k, \gamma_k\right) \end{bmatrix} \quad (2)
$$

$$
\overset{\text{def}}{=} \underbrace{\begin{bmatrix} \cos\phi_k\cos\theta_k & -\sin\phi_k \\ \sin\phi_k\cos\theta_k & \cos\phi_k \\ -\sin\theta_k & 0 \\ -\sin\phi_k & -\cos\phi_k\cos\theta_k \\ \cos\phi_k & -\sin\phi_k\cos\theta_k \\ 0 & \sin\theta_k \end{bmatrix}}_{\overset{\text{def}}{=}\Theta(\theta_k,\phi_k)} \underbrace{\begin{bmatrix} \sin\gamma_k e^{j\eta_k} \\ \cos\gamma_k \end{bmatrix}}_{\overset{\text{def}}{=}\boldsymbol{g}_k}
$$

$$
(3)
$$

where

$0 \leq \theta_k < \pi$ signal's elevation angle measured from the vertical z-axis;

$0 \leq \phi_k < 2\pi$ azimuth angle measured from the positive x-axis;

$0 \leq \gamma_k < \pi/2$ auxiliary polarization angle;

$-\pi \leq \eta_k < \pi$ polarization phase difference.

Note that $\Theta(\theta_k, \phi_k)$ depends only on the angular parameters, whereas $\boldsymbol{g}_k$ depends only on the polarizational parameters. For linearly polarized transverse electromagnetic waves $\eta_k = 0$; for circularly polarized waves, $\gamma_k = 45°$ and $\eta_k = \pm 90°$, + for left-circular polarization, and − for right-circular polarization.

There exist several essential observations about the electromagnetic vector sensor array-manifold. First, each single vector sensor possesses a 6×1 steering-vector and is effectively a six-element array in and of itself. Second, this electromagnetic vector sensor array-manifold contains no spatial phase factors as such; that is, the vector sensor array-manifold, unlike that of spatially displaced arrays, is *in*dependent of the impinging signal's frequency spectrum due to the spatial colocation of the

---

[3]This proposed algorithm may be modified to handle partially polarized or unpolarized signals by incorporating the technique in [30].

vector sensor's six constituent antennas. Third, the electromagnetic vector sensor array-manifold is polarization sensitive; that is, it is a function of $\{\gamma_k, \eta_k\}$. This means that signals having the same DOAs but different polarizations will have different array-manifolds and are thus distinguishable based on their polarization diversity. Fourth, any broad-band or narrow-band source's e_k and h_k^* are orthogonal to each other and to the source's normalized Poynting vector p_k, whose components simply constitute the three direction cosines along the three Cartesian coordinates

$$p_k \overset{\text{def}}{=} \begin{bmatrix} p_{x_k} \\ p_{y_k} \\ p_{z_k} \end{bmatrix} = \frac{e_k}{\|e_k\|} \times \frac{h_k^*}{\|h_k\|} = \begin{bmatrix} u_k \\ v_k \\ w_k \end{bmatrix} = \begin{bmatrix} \sin\theta_k \cos\phi_k \\ \sin\theta_k \sin\phi_k \\ \cos\theta_k \end{bmatrix} \tag{4}$$

where $*$ denotes complex conjugation $u_k \overset{\text{def}}{=} \sin\theta_k \cos\phi_k$, $v_k \overset{\text{def}}{=} \sin\theta_k \sin\phi_k$, and $w_k \overset{\text{def}}{=} \cos\theta_k$, respectively, represent the direction-cosines along the x-axis, the y-axis and the z-axis. This normalized Poynting vector uniquely determines the source's DOA. Thus, if the array-manifolds of all impinging sources can be estimated from the received data, then the signal-of-interests' DOA's can be estimated by performing the above vector cross product. After that, it would also be possible to estimate the signals' polarization states.

The spatial phase factor for the kth narrow-band[4] incident source to the lth vector-sensor located at (x_l, y_l, z_l) equals

$$q_l(u_k, v_k) \overset{\text{def}}{=} e^{j2\pi((x_l u_k + y_l v_k + z_l w_k)/\lambda)}$$
$$= \underbrace{e^{j2\pi(x_l u_k/\lambda)}}_{\overset{\text{def}}{=} q_l^x(u_k)} \underbrace{e^{j2\pi(y_l v_k/\lambda)}}_{\overset{\text{def}}{=} q_l^y(v_k)} \underbrace{e^{j2\pi(z_l w_k/\lambda)}}_{\overset{\text{def}}{=} q_l^z(w_k)}. \tag{5}$$

The kth signal impinging upon the lth vector sensor at time t produces the six-component vector measurement:[5]

$$a(\theta_k, \phi_k, \gamma_k, \eta_k) s_k(t) q_l(u_k, v_k) \tag{6}$$

where

$$s_k(t) \overset{\text{def}}{=} \sqrt{\mathcal{P}_k} \sigma_k(t) e^{j(2\pi(c/\lambda)t + \varphi_k)} \tag{7}$$

with $\mathcal{P}_k$ the kth signal's power, $\sigma_k(t)$ a zero-mean unit-variance complex random process, λ the signals' wavelength, c the propagation speed, and φ_k the kth signal's uniformly-distributed random carrier phase.

With a total of $K \leq 5$ cochannel signals[6] and additive white noise at each dipole or loop, the lth vector sensor produces the 6×1 vector measurement

$$z_l(t) = \sum_{k=1}^{K} \underbrace{a(\theta_k, \phi_k, \gamma_k, \eta_k) q_l(\theta_k, \phi_k)}_{\overset{\text{def}}{=} a_l(\theta_k, \phi_k, \gamma_k, \eta_k)} s_k(t) + n_l(t)$$
$$l = 1, \ldots, L. \tag{8}$$

For the entire arbitrarily spaced L-element electromagnetic vector-sensor array,[7] there exists a $6L \times 1$ vector measurement at each t

$$z(t) \overset{\text{def}}{=} \begin{bmatrix} z_1(t) \\ \vdots \\ z_L(t) \end{bmatrix}$$
$$= \sum_{k=1}^{K} s_k(t) q(u_k, v_k) \otimes a(\theta_k, \phi_k, \gamma_k, \eta_k) + n(t)$$
$$= As(t) + n(t) \tag{9}$$

where $\otimes$ denotes the Kronecker product and A represents the $6L \times K$ matrix

$$A \overset{\text{def}}{=} [q_l(u_1, v_1) \otimes a(\theta_1, \phi_1, \gamma_1, \eta_1), \ldots,$$
$$q_l(u_K, v_K) \otimes a(\theta_K, \phi_K, \gamma_K, \eta_K)] \tag{10}$$

$$s(t) \overset{\text{def}}{=} \begin{bmatrix} s_1(t) \\ \vdots \\ s_K(t) \end{bmatrix}; \quad n(t) \overset{\text{def}}{=} \begin{bmatrix} n_1(t) \\ \vdots \\ n_L(t) \end{bmatrix}$$
$$q(u_k, v_k) \overset{\text{def}}{=} \begin{bmatrix} e^{j2\pi(x_1 u_k + y_1 v_1 + z_1 w_k/\lambda)} \\ \vdots \\ e^{j2\pi(x_L u_k + y_L v_k + z_L w_k/\lambda)} \end{bmatrix} \tag{11}$$

where $n_l(t)$ symbolizes the 6×1 complex-valued zero-mean additive white noise vector at the lth vector sensor. With a total of $N > K$ snapshots taken at the distinct times $\{t_n, n = 1, \ldots, N\}$, the present electromagnetic vector-sensor DF problem[8] is to determine all $\{\theta_k, \phi_k, k = 1, \ldots, K\}$ from the $6L \times N$ data set

$$Z \overset{\text{def}}{=} \begin{bmatrix} Z_1 \\ \vdots \\ Z_L \end{bmatrix} = \begin{bmatrix} z_1(t_1) & \ldots & z_1(t_N) \\ \vdots & & \vdots \\ z_L(t_1) & \ldots & z_L(t_N) \end{bmatrix} \tag{12}$$

where each of the L submatrices Z_l of size $6 \times N$ corresponds to measurements at the lth electromagnetic vector sensor.

---

[4]These incident signals are narrow-band in that their bandwidths are very small compared to the inverses of the wavefronts' transit times across the array. The case involving broad-band signals may be reduced to a set of narrow-band problems using a comb of narrow-band filters.

[5]While the following electromagnetic vector-sensor model has not accounted for mutual coupling among the vector sensor's six component antennas, this model has been reported by Flam and Russell to be a very good approximation of their superCART array implementation of the vector-sensor concept. According to R. Flam (Flam and Russell, Inc., Horsham, PA) in a private correspondence to the first author on January 15, 1997, "...the patterns of the loops and dipoles [of the superCART array] are EXTREMELY close to the theoretical patterns, indicating very good isolation and balance among the elements."

[6]The above $K \leq 5$ maximum limit on the number of sources may readily be increased to $6\bar{L} - 1$ by replacing each vector sensor with a subarray of $\bar{L}$ vector sensors. Such subarrays may be arbitrarily configured so long as the same subarray configuration is used at all locations. This extension will be discussed in detail in the next section.

[7]While the preceding algorithmic development has assumed that all L vector sensors are identically oriented, a simple correctional procedure is presented in [35] to accommodate any nonidentical orientation among the L vector sensors.

[8]Although the proposed algorithm is presented in the batch processing mode, real-time adaptive implementations of this present algorithm may be readily realized for nonstationary environments using fast recursive eigendecomposition updating methods such as that in [15]. This proposed scheme may also be modified for tracking; see [33].

III. DIRECTION-FINDING WITH SELF-INITIATING MUSIC IN SPATIO-POLARIZATIONAL BEAMSPACE

A. Eigendecomposition of Collected Data

In eigenstructure (subspace) direction finding methods such as MUSIC, the overall data correlation matrix $\boldsymbol{Z}\boldsymbol{Z}^H$ (which embodies a maximum likelihood (ML) estimate of the true sample autocorrelation matrix if the additive noise is Gaussian) is decomposed into a K-dimensional signal subspace and a $(L - K)$-dimensional noise subspace. The first step in the proposed algorithm is to compute the K ($6L \times 1$) signal-subspace eigenvectors by eigendecomposing the $6L \times 6L$ data correlation matrix. Let $\boldsymbol{E}_s$ represent the $6L \times K$ matrix composed of the K eigenvectors corresponding to the K largest eigenvalues of the $6L \times 6L$ sample correlation matrix $\boldsymbol{Z}\boldsymbol{Z}^H$;[9] and let $\boldsymbol{E}_n$ denote the $6L \times (6L - K)$, matrix composed of the remaining $6L - K$ eigenvectors of $\boldsymbol{Z}\boldsymbol{Z}^H$

$$
\begin{aligned}
\boldsymbol{R}_{zz} = \boldsymbol{Z}\boldsymbol{Z}^H &= \frac{1}{N} \sum_{i=1}^{N} \boldsymbol{z}(t_i) \boldsymbol{z}^H(t_i) \\
&= \boldsymbol{E}_s \boldsymbol{D}_s \boldsymbol{E}_s^H + \boldsymbol{E}_n \boldsymbol{D}_n \boldsymbol{E}_n^H
\end{aligned} \tag{13}
$$

where

$$
\begin{aligned}
\boldsymbol{E}_s &\approx \boldsymbol{A}\boldsymbol{T} \\
&= [\boldsymbol{q}(u_1, v_1) \otimes \boldsymbol{a}(\theta_1, \phi_1, \gamma_1, \eta_1), \ldots, \\
&\quad \boldsymbol{q}(u_K, v_K) \otimes \boldsymbol{a}(\theta_K, \phi_K, \gamma_K, \eta_K)] \boldsymbol{T}
\end{aligned} \tag{14}
$$

$\boldsymbol{D}_s$ symbolizes a $K \times K$ diagonal matrix whose diagonal entries embody the K largest eigenvalues and $\boldsymbol{D}_n$ represents a $(6L - K) \times (6L - K)$ diagonal matrix whose diagonal entries contain the $6L - K$ smallest eigenvalues and $\boldsymbol{T}$ denotes an unknown but nonsingular $K \times K$ coupling matrix. $\boldsymbol{T}$ is nonsingular because both $\boldsymbol{E}_s$ and $\boldsymbol{A}$ are full rank. If there exists no noise or if an infinite number of snapshots are available, the approximation in (14) will become an exact identity.

B. Blind Spatio-Polarizational Beamforming

LCMV [1] is a statistically optimal beamforming technique that allows extensive control of beamformer response by a set of linear constraints, which may be set 1) to pass (with specified gain and phase) signals from favored directions and polarizations or to block interferences from other directions and polarizations and 2) to minimize output variance. LCMV beamforming produces a specified set of spatial angular peaks and nulls much like setting a finite impulse response (FIR) filter's coefficients to produce a specified set of spectral peaks and nulls. Regardless of the overall array geometry, an identical LCMV spatio-polarization beamformer is realizable at each individual vector-sensor using the electromagnetic-field estimates derived in (25).

This spatio-polarizational beamforming reduces MUSIC's four-dimensional search (over the azimuth, the elevation, the auxiliary polarization angle and the polarization phase difference) to only a two-dimensional (2-D) search over the two

DOA parameters, thereby decoupling the polarization parameters estimation problem from the direction finding problem. Furthermore, spatio-polarizational beamforming nulls out all but the signal-of-interest and thus removes those optima in the MUSIC spectrum corresponding to the interfering sources. This facilitates speedy convergence to the MUSIC spectrum's global optimum. While data size has already been reduced from $6L \times N$ to $6L \times K$ in the eigendecomposition step at (13) and (14), spatio-polarizational beamforming further reduces the data size to $L \times K$.

The LCMV beamformer weights passing the kth source but nulling all other $K - 1$ sources may be derived as

$$
\boldsymbol{w}_k = R_{vs}^{-1} \boldsymbol{C}^H \left(\boldsymbol{C} R_{vs}^{-1} \boldsymbol{C}^H \right)^{-1} \boldsymbol{e}_k \tag{15}
$$

where

$$
\boldsymbol{R}_{vs} \stackrel{\text{def}}{=} \sum_{k=1}^{K} \hat{\boldsymbol{a}}_k \hat{\boldsymbol{a}}_k^H \tag{16}
$$

$$
\boldsymbol{C} \stackrel{\text{def}}{=} \left[\hat{\boldsymbol{a}}_1 \vdots \ldots \vdots \hat{\boldsymbol{a}}_K \right] \tag{17}
$$

where $\hat{\boldsymbol{a}}_k$ is the estimate of $\boldsymbol{a}(\theta_k, \phi_k, \gamma_k, \eta_k)$, and $\boldsymbol{e}_k$ denotes a $K \times 1$ vector with all zeros except a one at the kth position to signal that only the kth source is to be passed. The K columns of the constraint matrix $\boldsymbol{C}$ simply correspond to the K sources' estimated steering vectors. $\boldsymbol{w}_k$ minimizes $\boldsymbol{w}_k^H \boldsymbol{R}_{vs} \boldsymbol{w}_k$ (i.e., the output variance or power) while satisfying the constraint $\boldsymbol{C}^H \boldsymbol{w}_k = \boldsymbol{e}_k$. These vector sensor polarized beams have been formed with no explicit estimation of either the polarization parameters or the arrival angles.

This 6×1 LCMV polarized-beamforming weight vector $\boldsymbol{w}_k$ is to be applied identically to each $6 \times K$ sector of the $6L \times K$ signal-subspace eigenvector matrix of (14)

$$
\boldsymbol{E}_{b_k} \stackrel{\text{def}}{=} \left(\boldsymbol{I}_L \otimes \boldsymbol{w}_k^H \right) \boldsymbol{E}_s \tag{18}
$$

where $\boldsymbol{I}_L$ refers to an $L \times L$ identity matrix and $\boldsymbol{E}_{b_k}$ denotes the kth source's $L \times K$ polarized beamformer output, passing only the kth source but nulling all other $K - 1$ sources. Note that each signal-of-interest has its own $\boldsymbol{w}_k$ and, thus, its own $\boldsymbol{E}_{b_k}$ plus its own 2-D iterative search. This $L \times K$ polarized-beamformer output is to be used in a 2-D DOA search to be discussed in the next subsection.

The impinging sources' spatial diversity (in additional to their polarization diversity) is exploited by this uni-vector-sensor-based beamformer in a way fundamentally different from the situation with a conventional phased array of scalar sensors. In the latter case, the sources' spatial diversity is encapsulated in the spatial phase-factors between the phased-array's spatially displaced antennas. In contrast, no spatial phase-factors, as such, exist among the vector-sensor's component-antennas because all six component-antennas are spatially colocated—though the vector sensor's six-component manifold, a function of the elevation angle and the azimuth angle, implicitly depends on the values of the spatial phase factors. The Vandermonde structure in the array manifold of a uniformly spaced array of identical scalar-sensors no longer exists with*in* a vector sensor. Instead, the sources' spatial diversity is directly encapsulated in the vector sensor through the complex scalar response of each of

---

[9]The value of K (i.e., the number of impinging sources) may be estimated based on the magnitude distribution of the eigenvalues of $\boldsymbol{Z}\boldsymbol{Z}^H$ using various model selection criteria such as that in [18].
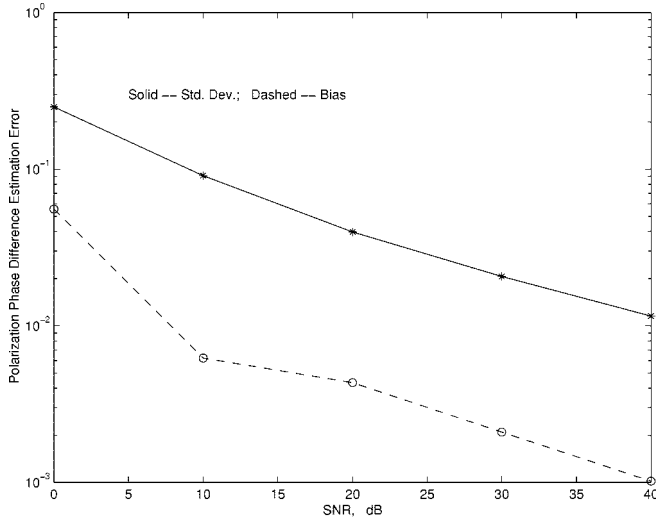
Fig. 1. The rms standard deviation of $\{\hat{u}_1, \hat{v}_1, \hat{u}_2, \hat{v}_2\}$ versus SNR: two closely spaced equal-power uncorrelated narrow-band incident sources, 100 snapshots per experiment, 300 independent experiments per data point.

Fig. 2. The rms bias of $\{\hat{u}_1, \hat{v}_1, \hat{u}_2, \hat{v}_2\}$ versus SNR: same settings as in Fig. 1.

the six component antennas. Uni-vector-sensor beamforming, thus, embodies a kind of electromagnetic-field weighting, distinct from the phased-array's spatial-filtering. Note also that *spatial* beamforming techniques [3], [5], [7] mentioned earlier can be applied to further reduce the dimension of this $L \times K$ polarized-beamspace data set when *a priori* information on the incident sources are available.

C. Estimation of Electromagnetic Vector-Sensor Steering Vectors

The previously developed blind beamforming procedure needs $\{\hat{a}_k, k = 1, \ldots, K\}$, which are to be derived using ESPRIT [4]. ESPRIT here exploits the translational invariance between two translationally displaced vector sensors. Altogether $L(L-1)/2$ different possible pairs of vector sensors may be formed out of the L vector sensors. Each of these $L(L-1)/2$ ESPRIT vector sensor pairs produces its own estimate of $\{a(\theta_k, \phi_k, \gamma_k, \eta_k), k = 1, \ldots, K\}$, which must then be summed coherently to preserve signal power while and to enhance noise cancellation.

Available at this point of the algorithm are the K number of $6L \times 1$ signal-subspace eigenvectors (14), from which the lth vector-sensor's K 6×1 signal-subspace eigenvectors may be extracted

$$E_l \stackrel{\text{def}}{=} (e_l \otimes I_6) E_s \qquad (19)$$
$$\approx [q_l(u_1, v_1) a(\theta_1, \phi_1, \gamma_1, \eta_1), \ldots,$$
$$q_l(u_K, v_K) a(\theta_K, \phi_K, \gamma_K, \eta_K)] T \qquad (20)$$
$$\approx [a(\theta_1, \phi_1, \gamma_1, \eta_1), \ldots, a(\theta_K, \phi_K, \gamma_K, \eta_K)]$$
$$\cdot Q_l(u_1, \ldots, u_K, v_1, \ldots, v_K) T \qquad (21)$$

$$Q_l(u_1, \ldots, u_K, v_1, \ldots, v_K)$$
$$\stackrel{\text{def}}{=} \begin{bmatrix} q_l(u_1, v_1) & & \\ & \ddots & \\ & & q_l(u_K, v_K) \end{bmatrix} \qquad (22)$$
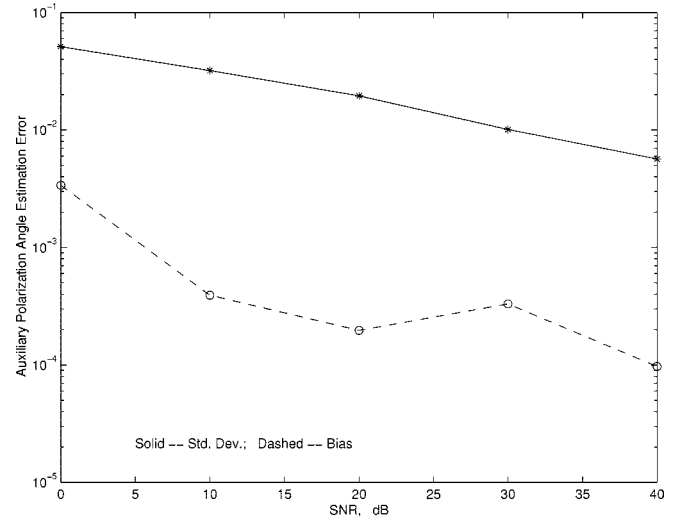
where e_l symbolizes a $1 \times L$ vector with all zeros except a one in the lth position and I_6 denotes a 6×6 identity matrix.

An ESPRIT matrix pencil pair involving the ith and the jth vector-sensor may be constructed using the two $6 \times K$ matrices E_i and E_j, both of which, being full rank, are related by a $K \times K$ nonsingular matrix Ψ_{ij}

$$E_i \Psi_{ij} = E_j \qquad (23)$$
$$\Rightarrow \Psi_{ij} = (E_i^H E_i)^{-1} (E_i^H E_j) = T_{ij}^{-1} \Phi_{ij} T_{ij}$$
$$= (P_{ij} T_{ij})^{-1} \tilde{\Phi}_{ij} (P_{ij} T_{ij}) \qquad (24)$$

where

P_{ij} $K \times K$ permutation matrix;
Φ_{ij} diagonal matrix whose diagonal element;
$[\Phi_{ij}]_{kk}$ eigenvalue of Ψ_{ij} with a corresponding eigenvector equal to the kth column of T_{ij}^{-1};
T_{ij} estimate of T using data from the ith and the jth vector-sensors;
$\tilde{\Phi}_{ij}$ Φ_{ij} except a re-ordering of the diagonal elements.

The above eigendecomposition of Ψ_{ij} can only determine T_{ij}^{-1} to within some column permutation. This is because (24) still holds replacing T_{ij} and Φ_{ij}, respectively, by $P_{ij} T_{ij}$ and $P_{ij} \Phi_{ij} (P_{ij})^{-1}$, hence, the presence of the $K \times K$ permutation matrix P_{ij} on the right-hand sides of the equation. ESPRIT may be concurrently applied to these $L(L-1)/2$ matrix pencil pairs via parallel computation.

In order to sum these $L(L-1)/2$ estimates of the K steering vectors, the permutational ambiguities associated with $\{P_{ij}, 1 \geq i < j \geq L\}$ must next be resolved. That is, P_{ij} must be estimated. As $P_{ij} T_{ij}$ embodies a unitary matrix, the rows of $P_{ij} T_{ij}$ constitute an orthogonal set. Let l_k denotes the row index of the matrix element with the largest absolute value in the kth column of the $K \times K$ matrix $(P_{mn} T_{mn})(P_{ij} T_{ij})^{-1}$. Then the l_kth row of $P_{mn} T_{mn}$ must correspond to the lth row of $P_{ij} T_{ij}$. This pairing procedure requires *no* exhaustive searches and thus requires minimum computation.

Having thus permuted $\{P_{ij} T_{ij}, 1 \leq i < j \leq L\}$ to obtain $\{T_{ij}, 1 \leq i < j \leq L\}$, $\{E_l, 1 \leq l \leq L\}$ may now be decoupled and coherently summed to yield composite estimates
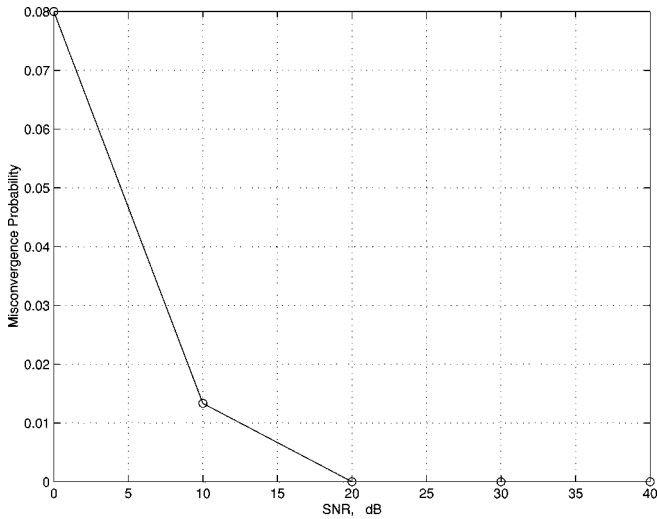
Fig. 3. The rms standard deviation and bias of $\{\hat{\eta}_1, \hat{\eta}_2\}$ (in radians) versus SNR: same settings as in Fig. 1.

$\{\hat{a}_k, k = 1, \ldots, K\}$ of the K six-component electromagnetic-field vectors

$$\hat{a}_k = \frac{\left[\displaystyle\sum_{1 \leq i < j \leq L} \left(E_i T_{ij}^{-1} + E_j T_{ij}^{-1} \Phi_{ij} \right) \Phi_{1i} \right] e_k}{\left\| \left[\displaystyle\sum_{1 \leq i < j \leq L} \left(E_i T_{ij}^{-1} + E_j T_{ij}^{-1} \Phi_{ij} \right) \Phi_{1i} \right] e_k \right\|} \quad (25)$$

where $\Phi_{11} \overset{\text{def}}{=} I_2$ and e_k denotes a $K \times 1$ zero vector with a single one at the kth position. Φ_{ij} renders the summation of $E_i T_{ij}^{-1}$ and $E_j T_{ij}^{-1}$ coherent for any particular i and j. Computing all $L(L-1)/2$ matrix-pencil pairs enhances noise cancellation because that will utilize all data collected from all L vector sensors and exploits all spatial invariances among all L vector-sensors. However, it may be possible to economize on computation by applying ESPRIT to only a few of the $L(L-1)/2$ possible pairs at the cost of poorer sdecoupling of the sources' steering vectors and thus less accurate DOA coarse estimates and less effective source selectivity in LCMV beamforming. (i.e., poorer estimation of T and poorer separation of the steering vectors of the K sources.)

The coarse direction-cosine estimates $\{\hat{u}_k, \hat{v}_k, \hat{w}_k\}$ may now be obtained by a vector cross-product between each signals' electrical-field estimate and magnetic-field estimate

$$\begin{bmatrix} \hat{u}_k \\ \hat{v}_k \\ \hat{w}_k \end{bmatrix} = \hat{p}_k = \begin{bmatrix} \hat{p}_{x_k} \\ \hat{p}_{y_k} \\ \hat{p}_{z_k} \end{bmatrix} = \frac{\hat{e}_k}{\|\hat{e}_k\|} \times \frac{\hat{h}_k^*}{\|\hat{h}_k\|}. \quad (26)$$

In the more realistic scenario when noise is present and when only a finite number of snapshots are available, the above relations become only approximate.

As a side note, many of these $L(L-1)/2$ ESPRIT vector sensor pairs may possess an intervector sensor spacing in excess of an half wavelength. This will result in a cyclic ambiguity of some integer multiple of 2π in ESPRIT's eigenvalues' phases. The one-to-one mapping between ESPRIT's

eigenvalues' phase angles and the direction-cosines will no longer exist and no unambiguous direction cosine estimates can be obtainable from ESPRIT's eigenvalues. However, given that it is T, not ESPRIT's eigenvalues, which is needed in the algorithm, this cyclic ambiguity of ESPRIT's eigenvalues' phases is irrelevant to the objective on hand. ESPRIT, regardless of the intervector sensor spacing, can always estimate T_{ij} and Ψ_{ij}, which are all that matter. In other words, coarse direction-cosine initial estimates are herein derived not from ESPRIT's eigenvalues, as is often the case in other sensor array direction finding schemes in other ESPRIT-based algorithms, but from ESPRIT's signal-subspace eigenvectors. ESPRIT's eigenvalues are not usable because any or all of the intervector sensor separations may exceed the Nyquist half-wavelength maximum and some unknown cyclic ambiguities will thus exist in ESPRIT's eigenvalues. In contrast, ESPRIT's signal-subspace eigenvectors are usable because they suffer no ambiguity despite to extended intervector sensor spacing. Knowledge of these signal-subspace eigenvectors leads to direct estimation (via the vector cross-product estimator) of the direction-cosines because full electromagnetic field information is available in the vector sensor's manifold. If each vector sensor is replaced by a subarray of uniformly polarized but displaced scalar sensors, the present algorithm would not work. This is because the direction-cosine information cannot be easily extracted from the subarray manifold of a subarray of displaced but identically polarized sensors unless another MUSIC-like search is to be performed over the subarray manifold.

D. Spatio-Polarizational Beamspace Self-Initiating MUSIC-Based Direction Finding

Applying MUSIC to the LCMV spatio-polarizational beamformer output, the direction-cosine estimates for the kth source are

$$\{\hat{u}_k, \hat{v}_k\} \overset{\text{def}}{=} \underset{u, v}{\arg \max} \left\| E_{b_k}^H q(u, v) \right\|. \quad (27)$$

Note that unlike customary formulation of the MUSIC algorithm, the kth source's dimension-reduced signal-subspace steering vector, not the null-space eigenvectors, is used in the above optimization. This is because the null-space eigenvectors, being orthogonal to all $\{q(u_k, v_k), k = 1, \ldots, K\}$, contains "contaminating" information from the phase factors of the other K sources. In contrast E_{b_k}, as the output of LCMV interference rejection beamformer contains information only of the kth source. Thus, using E_{b_k} in (27) removes the interferers' spectral optima in the MUSIC spectrum, resulting in a flattened scalar function for optimization and, thus, faster convergence to more accurate arrival angle estimates. As a side note, customary formulations of MUSIC uses the null-space eigenvectors and not the signals' steering vectors in above optimization because the individual sources' steering vectors are unavailable. The signal-subspace eigenvector set (i.e., the columns of E_s) cannot ordinarily be decoupled into the K impinging sources' respective steering vectors. In contrast, this decoupling can be successfully performed using techniques described in the preceding subsections. Thus, the MUSIC-based search of this novel algorithm may use each individual array
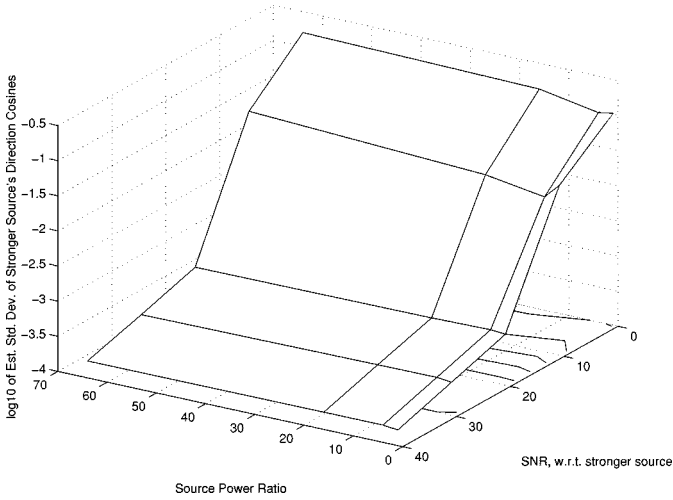
Fig. 4. The rms standard deviation and bias of $\{\hat{\gamma}_1, \hat{\gamma}_2\}$ (in radians) versus SNR: same settings as in Fig. 1.

source's manifold instead of the null-space eigenvectors as in identically polarized MUSIC's iterative search.

From the direction-cosine estimates derived above, the kth signal's azimuth and elevation arrival angles may be estimated as

$$\hat{\theta}_k = \sin^{-1} \sqrt{\hat{u}_k^2 + \hat{v}_k^2} = \cos^{-1} \hat{w}_k \quad (28)$$

$$\hat{\phi}_k = \angle \left(\hat{u}_k + j\hat{v}_k \right). \quad (29)$$

The corresponding polarization parameter estimates equal

$$\hat{\gamma}_k = \tan^{-1} \left\| \frac{\hat{g}_{k_1}}{\hat{g}_{k_2}} \right\| \quad (30)$$

$$\hat{\eta}_k = \angle \hat{g}_{k_1} - \angle \hat{g}_{k_2} \quad (31)$$

where

$$\hat{\boldsymbol{g}}_k = \begin{bmatrix} \hat{g}_{k_1} \\ \hat{g}_{k_2} \end{bmatrix}$$
$$\stackrel{\text{def}}{=} \left[\boldsymbol{\Theta}^H \left(\hat{\theta}_k, \hat{\phi}_k \right) \boldsymbol{\Theta} \left(\hat{\theta}_k, \hat{\phi}_k \right) \right]^{-1} \boldsymbol{\Theta}^H \left(\hat{\theta}_k, \hat{\phi}_k \right) \hat{\boldsymbol{a}}_k \quad (32)$$

and $\boldsymbol{\Theta}(\theta_k, \phi_k)$ has been defined in (3). Note that these estimates of the sources' azimuths, elevations, and polarization parameters have been automatically matched with no additional processing.

IV. EXTENSION TO IRREGULARLY SPACED SUBARRAYS OF ELECTROMAGNETIC VECTOR-SENSORS

This section extends the above developed scheme to accommodate more than five sources. This five-source constraint arises from the 6×1 size of an individual electromagnetic vector sensor's array manifold. This maximum may be raised to $6\tilde{L} - 1$ or $6L - 1$ by deploying at each of the L irregularly spaced location a subarray of $\tilde{L}$ vector-sensors instead of just one vector sensor. These subarrays may be arbitrarily configured so long as all subarrays at all locations are identical.

Consider L identical subarrays, each of which consists of $\tilde{L}$ vector-sensors, irregularly placed in a 3-D space. The overall $6\tilde{L}L \times 1$ array manifold for the kth incident source becomes

$$\boldsymbol{a}(\theta_k, \phi_k, \gamma_k, \eta_k) \stackrel{\text{def}}{=} \boldsymbol{q}(u_k, v_k) \otimes \underbrace{\begin{bmatrix} q_1^{\text{sub}}(u_k, v_k) \\ \vdots \\ q_{\tilde{L}}^{\text{sub}}(u_k, v_k) \end{bmatrix}}_{\stackrel{\text{def}}{=} \boldsymbol{q}^{\text{sub}}(u_k, v_k)}$$

$$\otimes \begin{bmatrix} e_x(\theta_k, \phi_k, \gamma_k, \eta_k) \\ e_y(\theta_k, \phi_k, \gamma_k, \eta_k) \\ e_z(\theta_k, \gamma_k, \eta_k) \\ h_x(\theta_k, \phi_k, \gamma_k, \eta_k) \\ h_y(\theta_k, \phi_k, \gamma_k, \eta_k) \\ h_z(\theta_k, \gamma_k) \end{bmatrix} \quad (33)$$

$$q_{\tilde{l}}^{\text{sub}}(u_k, v_k) \stackrel{\text{def}}{=} e^{j2\pi((x_{\tilde{l}}^{\text{sub}} u_k + y_{\tilde{l}}^{\text{sub}} v_k + z_{\tilde{l}}^{\text{sub}} w_k)/\lambda)} \quad (34)$$

where $(x_{\tilde{l}}^{\text{sub}}, y_{\tilde{l}}^{\text{sub}}, z_{\tilde{l}}^{\text{sub}})$ represents the location of the subarray's $\tilde{l}$th vector sensor *relative* to the subarray's first vector-sensor located at $(x_1^{\text{sub}}, y_1^{\text{sub}}, z_1^{\text{sub}})$. Thus, $q_1^{\text{sub}}(u_k, v_k) = 1$.

Developments in Section III and all equations from (2) to (32) still hold with the appropriate size changes and (19) to be modified as

$$\boldsymbol{E}_l = (\boldsymbol{e}_l \otimes \boldsymbol{I}_{6\tilde{L}}) \boldsymbol{E}_s \quad (35)$$

where $\boldsymbol{e}_l$ denotes a $1 \times L$ vector with all zeros except a one at the lth position. This $\boldsymbol{e}_l$ selects the lth-subarray sector of $\boldsymbol{E}_s$ as $\boldsymbol{E}_l$. (25) now produces the $6\tilde{L} \times 1$ subarray manifold estimates, from which the kth source's six electromagnetic-field components may be derived

$$\hat{\boldsymbol{a}}_k = \frac{\sum_{\tilde{l}=1}^{\tilde{L}} (\boldsymbol{e}_{\tilde{l}} \otimes \boldsymbol{I}_6) \left[\sum_{1 \le i < j \le L} \left(\boldsymbol{E}_i \boldsymbol{T}_{ij}^{-1} + \boldsymbol{E}_j \boldsymbol{T}_{ij}^{-1} \boldsymbol{\Phi}_{ij} \right) \boldsymbol{\Phi}_{1i} \right] \boldsymbol{e}_k}{\left\| \sum_{\tilde{l}=1}^{\tilde{L}} (\boldsymbol{e}_{\tilde{l}} \otimes \boldsymbol{I}_6) \left[\sum_{1 \le i < j \le L} \left(\boldsymbol{E}_i \boldsymbol{T}_{ij}^{-1} + \boldsymbol{E}_j \boldsymbol{T}_{ij}^{-1} \boldsymbol{\Phi}_{ij} \right) \boldsymbol{\Phi}_{1i} \right] \boldsymbol{e}_k \right\|} \quad (36)$$

(18) also becomes

$$\boldsymbol{E}_{b_k} \stackrel{\text{def}}{=} \left(\boldsymbol{I}_{L\tilde{L}} \otimes \boldsymbol{w}_k^H \right) \boldsymbol{E}_s. \quad (37)$$

The above modifications allow the proposed method to handle up to $6\tilde{L} - 1$ sources. If $L > \tilde{L}$, then up to $6L - 1$ can be accommodated if the above array configuration of $L\tilde{L}$ vector-sensors is viewed as $\tilde{L}$ identical but translated subarrays of L irregularly spaced vector-sensors.

V. SIMULATIONS

Simulation results in Figs. 1–11 verify the efficacy of the proposed self-initiating MUSIC-based direction finding and polarization estimation algorithm. In all figures, two closely spaced uncorrelated narrowband incident sources with the following parameter values: $\{\theta_1 = 59.1°, \phi_1 = 53.5°, \gamma_1 = 45°, \eta_1 = -90°\}$ and $\{\theta_2 = 59.1°, \phi_2 = 36.5°, \gamma_2 = 45°, \eta_2 = 90°\}$.

Fig. 5.   Misconvergence frequency versus SNR: same settings as in Fig. 1.

Fig. 6.   The rms standard deviation of $\{\hat{u}_1, \hat{v}_1\}$ versus SNR and $\mathcal{P}_1/\mathcal{P}_2$. Same scenario as in Fig. 1 except the value of $\mathcal{P}_2$.

That is, the signal-of-interest (with subscript 1) has $u_1 = 0.51$ and $v_1 = 0.69$ and is right-circularly polarized, and the interference (with subscript 2) has $u_2 = 0.69$ and $v_2 = 0.51$ and is left-circularly polarized. Thirteen identically oriented electromagnetic vector sensors are placed at the (x, y, z) coordinates

$$\frac{\lambda}{2} \times \{(0, 0, 0), (0, 1, 0), (0, 2.7, 0), (1, 0, 0), (2.7, 0, 0)$$
$$(0, -1, 0), (0, -2.7, 0), (-1, 0, 0), (-2.7, 0, 0),$$
$$(4, -4, 1), (4, 4, 1), (-4, -4, 1), (-4, 4, 1)\}$$

where λ refers to the sources' common wavelength. The additive white noise is complex Gaussian; and the SNR is defined relative to each source. One-hundred snapshots are used in each of the 300 independent Monte Carlo simulation experiments. The estimation error in each experiment is computed by finding the difference between $\{\hat{u}, \hat{v}\}$. The Nelder–Meade simplex algorithm is used in the iterative searches. In Figs. 1–5, the two sources have equal power, whereas in Figs. 6–11, $\mathcal{P}_1/\mathcal{P}_2$ varies from unity to 64. $L-1 = 12$ TLS-ESPRIT[10] matrix pencil pairs, those involving the $(0, 0, 0)$ vector sensor and each of the other 12, estimate the Poynting vector.

Figs. 1 and 2 respectively plot the direction-cosines' composite estimation standard deviation and bias versus SNR for $\mathcal{P}_1 = \mathcal{P}_2$. The composite root mean square (rms) standard deviation equals the square root of the mean of the respective samples variances of $\{\hat{u}_1, \hat{v}_1, \hat{u}_2, \hat{v}_2\}$; the composite bias equals the square root of the mean of the square of the respective sample biases of $\{\hat{u}_1, \hat{v}_1, \hat{u}_2, \hat{v}_2\}$. Fig. 3 plots the composite rms standard deviation and bias of $\{\hat{\eta}_1, \hat{\eta}_2\}$ versus SNR. Fig. 4 plot the composite rms standard deviation and bias of $\{\hat{\gamma}_1, \hat{\gamma}_2\}$ versus SNR. All four figures follow similar trends. Because $u_2 - u_1 = v_1 - v_2 = 0.18$, the two sources are resolved and identified with high probability if both the estimation standard deviation and the bias are under approximately 0.06. Referring to these two figures, the proposed blind algorithm successfully

---

[10]TLS-ESPRIT [4] represents a total-least squares (TLS) realization of the ESPRIT algorithm. TLS-ESPRIT recognizes that both subarrays, rather than just one subarray, are corrupted by noise.
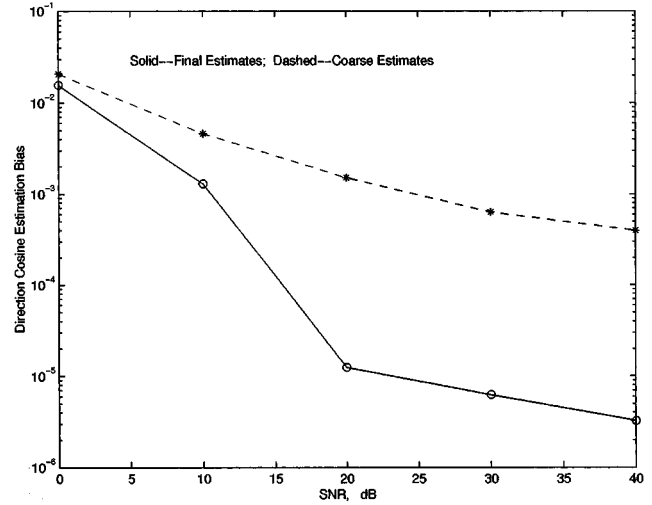

Fig. 7.   The rms bias of $\{\hat{u}_1, \hat{v}_1\}$ versus SNR and $\mathcal{P}_1/\mathcal{P}_2$. Same scenario as in Fig. 1 except the value of $\mathcal{P}_2$.

Fig. 8.   The rms standard deviation of $\{\hat{u}_2, \hat{v}_2\}$ versus SNR and $\mathcal{P}_1/\mathcal{P}_2$. Same scenario as in Fig. 1 except the value of $\mathcal{P}_2$.
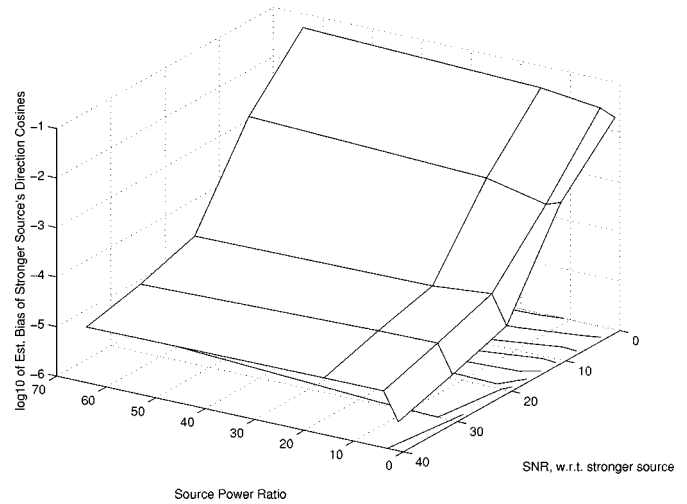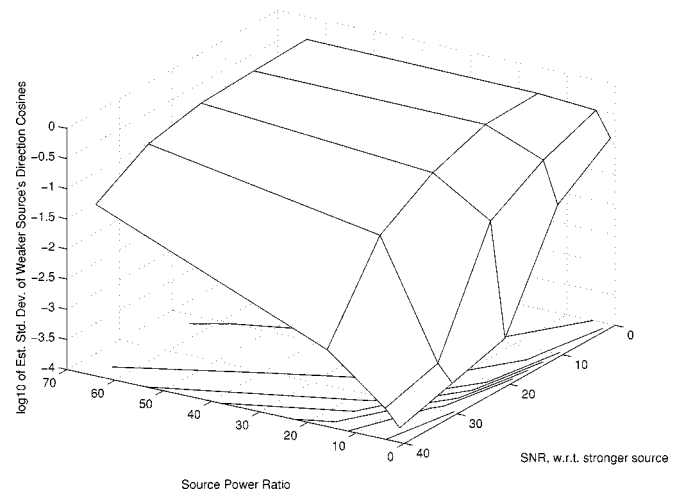
resolved these closely spaced sources for all SNRs above 2 dB without any *a priori* information on the sources' DOAs.
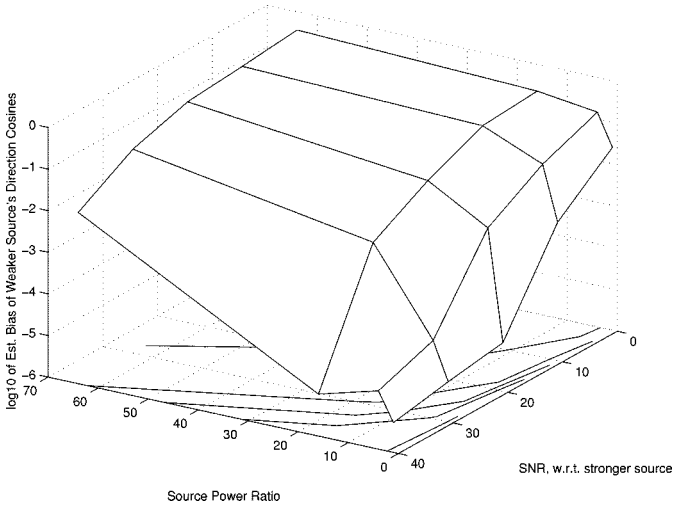
Fig. 9. The rms bias of $\{\hat{u}_2, \hat{v}_2\}$ versus SNR and $\mathcal{P}_1/\mathcal{P}_2$. Same scenario as in Fig. 1 except the value of $\mathcal{P}_2$.

Fig. 11. The weaker source's misconvergence frequency versus SNR and $\mathcal{P}_1/\mathcal{P}_2$. Same scenario as in Fig. 1 except the value of $\mathcal{P}_2$.
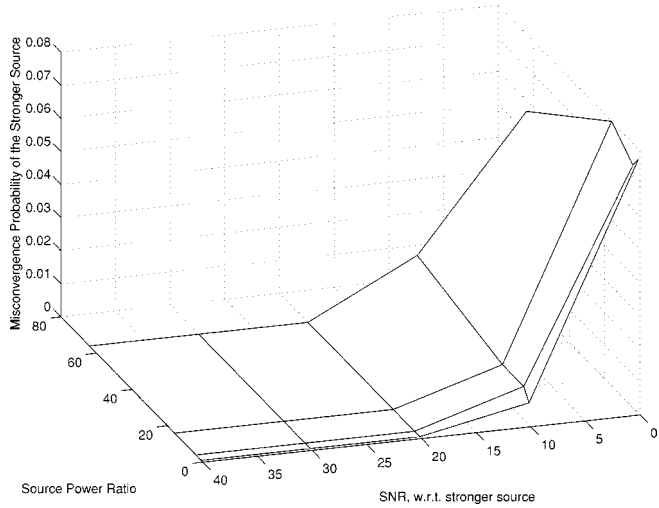

Fig. 10. The stronger source's misconvergence frequency versus SNR and $\mathcal{P}_1/\mathcal{P}_2$. Same scenario as in Fig. 1 except the value of $\mathcal{P}_2$.

Fig. 1 also shows the closeness of the proposed algorithm's performance to the Cramer–Rao bound (CRB). for SNR at or above 20 dB.

Very occasionally, the iterative search in Section III fails to converge to the intended source specified by the coarse estimate. Fig. 5 shows that misconvergence happens at only SNR's below 20 dB and remains under 2% down to 10 dB. Misconvergence may be caused by imperfect decoupling of the signal-subspace eigenvectors and, thus, imperfectly formed LCMV beams block the interference only partially. MUSIC's iterative search then misconverges to a spectral optimum corresponding to an interfering source. This problem may be alleviated by using more ESPRIT matrix pencil pairs (instead of only $L-1$ pairs as in (25) to better decouple the signal-subspace eigenvectors. A more sophisticated search algorithm than the the Nelder-Meade simplex algorithm (implemented in MATLAB as "fmins") may also converge better.

Figs. 6–11 plot the estimation performance when the first source has higher power than the second source. The SNR is defined with reference to the stronger source's power. Figs. 6
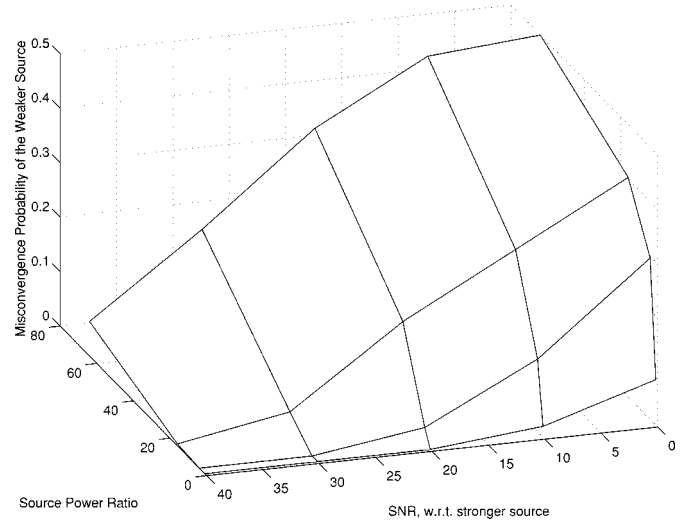
and 7, respectively, plot the rms standard deviation and bias for the first source, whereas Figs. 8 and 9 do the same for the weaker source. Figs. 10 and 11 plot the misconvergence frequency for the stronger source and the weaker source, respectively. It may be observed that while the stronger source is little affected by the weaker source's power level, misconvergence tends toward a major problem for the weaker source at large $\mathcal{P}_1/\mathcal{P}_2$ and small SNR.

VI. CONCLUSION

This novel MUSIC-based direction finding method recognizes the impinging electromagnetic wavefield as a diversely polarized *vector* field instead of a mere intensity field. By deploying electromagnetic vector sensors instead of uniformly polarized antennas, spatio-polarization beams may be formed to remove false optima in MUSIC's cost function and to decouple the DOA estimation problem from the polarization parameter estimation problem, resulting in two degrees of dimensionality reduction in MUSIC's optimization procedure. Moreover, the sources' DOAs are estimated through the vector cross-product, rather than through estimating interelement spatial phase delays as customarily done. This vector cross-product DOA estimator supplies coarse direction-cosine estimates to start off the MUSIC-based iterative search over the intervector sensor spatial phase-delay array manifold with*out* any *a priori* information of the sources' parameters, thereby facilitating *faster* convergence to the *global* optimum. Simulation results verify the efficacy of the proposed method. While the preceding algorithmic development has assumed that all L vector sensors are identically oriented, a simple correctional procedure is presented in [35] to accommodate any nonidentical orientation amongst the L vector sensors. Partially polarized signals may be handled by incorporating the technique in [30]. Techniques in [31] allows the substitution of the six-component vector sensor by the dipole triad or the loop triad, while preserving the efficacy of the presently proposed scheme. Although the algorithm is herein developed in the batch processing mode, real-time adaptive implementation for nonstationary environments is possible by incorporating the

techniques in [15], [34]. An underwater acoustic analog of the present scheme is available in [33] using underwater acoustical particle velocity hydrophones.

Numerous electromagnetic issues, however, remain to be addressed before the present signal processing scheme may become deployable. For example, reflection of the incident signals off the ground has not been addressed, though such multipaths may be decorrelated by spatial smoothing and thus be treated as additional incident signals. Mutual coupling across vector sensors presents another issue. Furthermore, The vector sensor array's support structure may severely distort the electromagnetic field, unless extraordinary precautions are taken to communicate the signal in and out of the vector sensors. While optical fibers can transport power to the vector sensor and to carry signals out from the dipole/loop structure, it is technically challenging to embed the necessary couplers and converters in the vector sensors with only negligible distortion to the electromagnetic field. This problem is especially acute when subarrays of vector sensors are to be placed at each array grid point.

REFERENCES

[1] O. L. Frost, "An algorithm for linearly constrained adaptive array processing," *Proc. IEEE*, vol. 60, pp. 926–935, Aug. 1972.

[2] R. O. Schmidt, "Multiple emitter location and signal parameter estimation," *IEEE Trans. Antennas Propagat.*, vol. AP-34, no. 3, pp. 276–280, Mar. 1986.

[3] X. Xu and K. Buckley, "Statistical performance comparison of MUSIC in element-space and beam-space," in *IEEE Int. Conf. Acoust., Speech, Signal Processing*, 1989, pp. 2124–2127.

[4] R. Roy and T. Kailath, "ESPRIT-estimation of signal parameters via rotational invariance techniques," *IEEE Trans. Acoust., Speech, Signal Processing*, vol. 37, pp. 984–995, July 1989.

[5] H. Lee and M. Wengrovitz, "Resolution threshold of beamspace MUSIC for two closely spaced emitters," *IEEE Trans. Acoust., Speech, Signal Processing*, vol. 38, pp. 1545–1559, Sept. 1990.

[6] D. J. Farina, "Superresolution compact array radiolocation technology (SuperCART) project," Flam Russell, Horsham, PA, Tech. Rep. 185, Nov. 1990.

[7] P. Stoica and A. Nehorai, "Comparative performance study of element-space and beam-space MUSIC estimators," *Circuits, Syst., Signal Processing*, vol. 10, no. 3, pp. 285–292, 1991.

[8] G. F. Hatke, "Performance analysis of the SuperCART antenna array," MIT Lincoln Laboratory, Cambridge, MA, Project Rep. #AST-22, Mar. 1992.

[9] G. F. Hatke, "Conditions for unambiguous source localization using polarization diverse arrays," in *27th Asilomar Conf.*, 1993, pp. 1365–1369.

[10] J. Li, "Direction and polarization estimation using arrays with small loops and short dipoles," *IEEE Trans. Antennas Propagat.*, vol. 41, pp. 379–387, Mar. 1993.

[11] A. Swindlehurst and M. Viberg, "Subspace fitting with diversely polarized antenna arrays," *IEEE Trans. Antennas Propagat.*, vol. 41, pp. 1687–1694, Dec. 1993.

[12] A. Nehorai and E. Paldi, "Vector-sensor array processing for electromagnetic source localization," in *Asilomar Conf.*, 1991, pp. 566–572.

[13] H. Lee and R. Stovall, "Maximum likelihood methods for determining the direction of arrival for a single electromagnetic source with unknown polarization," *IEEE Trans. Signal Processing*, vol. 42, pp. 474–478, Feb. 1994.

[14] J. F. Bull, "Field probe for measuring vector components of an electromagnetic field," U.S. Patent no. 5 300 885, Apr. 1994.

[15] B. Champagne, "Adaptive eigendecomposition of data covariance matrices based on first-order perturbations," *IEEE Trans. Signal Processing*, vol. 42, pp. 2758–2770, Oct. 1994.

[16] Q. Cheng and Y. Hua, "Performance analysis of the MUSIC and PENCIL-MUSIC algorithms for diversely polarized array," *IEEE Trans. Signal Processing*, vol. 42, pp. 3150–3165, Nov. 1994.

[17] K. A. Burgess and B. D. Van Veen, "A subspace GLRT for vector-sensor array detection," in *Proc. IEEE Int. Conf. Acoust., Speech, Signal Processing*, vol. 4, 1994, pp. 253–256.

[18] H. T. Wu,, J. F. Yang, and F. K. Chen, "Source number estimators using transformed Gerschgorin radii," *IEEE Trans Signal Processing*, vol. 43, pp. 1325–1333, June 1995.

[19] B. Hochwald and Nehorai, "Polarimetric modeling and parameter estimation with applications to remote sensing," *IEEE Trans. Signal Processing*, vol. 43, pp. 1923–1935, Aug. 1995.

[20] K.-C. Ho, K.-C. Tan, and W. Ser, "Investigation on number of signals whose directions-of-arrival are uniquely determinable with an electromagnetic vector sensor," *Signal Processing*, vol. 47, no. 1, pp. 41–54, Nov. 1995.

[21] B. Hochwald and A. Nehorai, "Identifiability in array processing models with vector-sensor applications," *IEEE Trans. Signal Processing*, vol. 44, no. 1, pp. 83–95, Jan. 1996.

[22] J. Li, P. Stoica, and D. Zheng, "Efficient direction and polarization estimation with a COLD array," *IEEE Trans. Antennas Propagat.*, vol. 44, pp. 539–547, Apr. 1996.

[23] K.-C. Tan, K.-C. Ho, and A. Nehorai, "Uniqueness study of measurements obtainable with arrays of electromagnetic vector sensors," *IEEE Trans. Signal Processing*, vol. 44, pp. 1036–1039, Apr. 1996.

[24] ——, "Linear independence of steering vectors of an electromagnetic vector sensor," *IEEE Trans. Signal Processing*, vol. 44, pp. 3099–3107, Dec. 1996.

[25] K. T. Wong and M. D. Zoltowski, "Uni-vector-sensor ESPRIT for multisource azimuth, elevation, and polarization estimation," *IEEE Trans. Antennas Propagat.*, vol. 45, pp. 1467–1474, Oct. 1997.

[26] ——, "Self-initiating MUSIC-based direction finding in polarization beamspace," in *Proc. Inst. Elect. Eng. Radar'97 Conf.*, 1997, IEE pub. #449, pp. 328–333.

[27] K.-C. Ho, K.-C. Tan, and B. T. G. Tan, "Efficient method for estimation of direction-of-arrival of partially polarized signals with electromagnetic vector sensors," *IEEE Trans. Signal Processing*, vol. 45, pp. 2485–2498, Oct. 1997.

[28] K. T. Wong, "Adaptive geolocation & blind beamforming for wideband fast frequency-hop signals of unknown hop sequences and unknown arrival angles using an electromagnetic vector-sensor," *Proc. IEEE Int. Conf. Commun.*, vol. 2, pp. 758–762, 1998.

[29] A. Nehorai, K.-C. Ho, and B. T. G. Tan, "Minimum-noise-variance beamformer with an electromagnetic vector sensor," *IEEE Trans. Signal Processing*, vol. 47, pp. 601–618, Mar. 1999.

[30] K. T. Wong, "Geolocation for partially polarized electromagnetic sources using multiple sparsely and uniformly spaced spatially stretched vector sensors," in *Proc. IEEE Int. Conf. Circuits Syst.*, vol. 3, 1999, pp. 170–174.

[31] ——, "A novel closed-form azimuth/elevation angle and polarization estimation technique using only electric dipole triads or only magnetic loop triads with arbitrary unknown spacings," in *Proc. IEEE Int. Conf. Circuits Syst.*, vol. 3, 1999, pp. 207–210.

[32] K.-C. Ho, K.-C. Tan, and A. Nehorai, "Estimating directions of arrival of completely and incompletely polarized signals with electromagnetic vector sensors," *IEEE Trans. Signal Processing*, vol. 47, pp. 2845–2852, Oct. 1999.

[33] A. Nehorai and P. Tichavsky, "Cross-product algorithms for source tracking using an EM vector sensor," *IEEE Trans. Signal Processing*, vol. 47, pp. 2863–2867, Oct. 1999.

[34] K. T. Wong and M. D. Zoltowski, "Self-initiating velocity-field beamspace MUSIC for underwater acoustic direction-finding with irregularly spaced vector-hydrophones," *IEEE J. Ocean. Eng.*, pp. 262–273, Apr. 2000.

[35] ——, "Closed-form direction-finding with arbitrarily spaced electromagnetic vector-sensors at unknown locations," *IEEE Trans. Antennas Propagat.*, vol. 48, pp. 671–681, May 2000.

[36] K. T. Wong and M. D. Zoltowski, "ESPRIT-based 2-D direction finding with a sparse uniform array of electromagnetic vector-sensors" (in *IEEE Trans. Signal Processing*, vol. 48, pp. 2195–2204, Aug. 2000), in *IEEE Intl. Conf. Acoustics, Speech, Signal Processing*, vol. 5, 1996, pp. 2789–2792.

[37] M. D. Zoltowski and K. T. Wong, "Closed-form eigenstructure-based direction finding using arbitrary but identical subarrays on a sparse uniform Cartesian array grid," *IEEE Trans. Signal Processing*, vol. 48, pp. 2205–2210, Aug. 2000.

[38] A. Nehorai and E. Paldi, "Vector-sensor array processing for electromagnetic source localization," *IEEE Trans. Signal Processing*, vol. 42, pp. 376–398, Feb. 1994.

Kainam Thomas Wong (S'85–M'87) received the B.S. degree in chemical engineering from the University of Calfornia, Los Angeles, in 1985, the B.S.E.E. degree from the University of Colorado, Boulder, in 1987, the M.S.E.E. degree from Michigan State University, East Lansing, in 1990, and the Ph.D. degree in electrical engineering from Purdue University, West Lafayette, in 1996.

He was a Manufacturing Engineer at the General Motors Technical Center, Warren, MI, from 1990 to 1991, a Senior Professional Staff Member in the Applied Physics Laboratory, Johns Hopkins University, Laurel, MD, from 1996 to 1998, and has been an Assistant Professor in the Department of Electronic Engineering, Chinese University of Hong Kong, since August 1998. He is a contributing author of about 70 articles for the telecommunications section of the inaugural edition (2000) of the *CRC Dictionary of Pure and Applied Physics* and the *CRC Comprehensive Dictionary of Physics*. His current research interests are signal processing for communications and sensor array signal processing.

Dr. Wong serves on the Technical Program Committees of the 1999 and 2000 IEEE Wireless Communications and Networking Conference (WCNC'99, WCNC'00), the 1999 IEEE International Workshop on Intelligent Signal Processing and Communication Systems (ISPAC'99), the EuroComm 2000 Conference, and the 2000 Spring IEEE Vehicular Technology Conference (VTC'00 Spring). He also serves on the Organizing Committees of the 2000 IEEE International Symposium on Circuits Systems (ISCAS'00) and the Symposium 2000 on Adaptive Signal Processing, Communications and Control (AS-SPCC).

Michael D. Zoltowski (S'79–M'86–SM'95–F'99) was born in Philadelphia, PA, on August 12, 1960. He received both the B.S. and M.S. degrees in electrical engineering (with highest honors) from Drexel University, Philadelphia, in 1983 and the Ph.D. degree in systems engineering from the University of Pennsylvania, Philadelphia, in 1986.

From 1982 to 1986, he was an Office of Naval Research Graduate Fellow. During 1987, he held the position of Summer Faculty Research Fellow at the Naval Ocean Systems Center, San Diego, CA. In fall 1986, he joined the faculty of Purdue University, West Lafayette, IN, where he is currently a Professor of electrical and computer engineering. He has also served as a consultant to the General Electric Company. He is a contributing author to *Adaptive Radar Detection and Estimation* (New York: Wiley, 1991), *Advances in Spectrum Analysis and Array Processing, Vol. III* (Englewood, NJ: Prentice-Hall, 1994), and the *CRC Handbook on Digital Signal Processing* (Boca Raton, FL: CRC, 1996). His current research interests include space–time adaptive processing and blind antenna array beamforming for all areas of mobile and wireless communications, radar, and global positioning systems.

Dr. Zoltowski was the recipient of the IEEE Outstanding Branch Counselor Award 1989–1990 and the Ruth and Joel Spira Outstanding Teacher Award 1990–1991. He was the recipient of the IEEE Signal Processing Society 1991 Paper Award (statistical signal and array processing technical area). He was an Associate Editor for the IEEE TRANSACTIONS ON SIGNAL PROCESSING and is presently an Associate Editor for the IEEE COMMUNICATIONS LETTERS. He is a member of the IEEE Signal Processing Society Technical Committee for the Statistical Signal and Array Processing Area and a member of the Educational Committee.